ASPECTS OF THE ROTOR DESIGN FOR AXIALLY LAMINATED SYNCHRONOUS RELUCTANCE MOTORS

X. Feng, K. Hameyer and R. Belmans
E. E. Dept., Div. ESAT/ELEN, Katholieke Universiteit Leuven
Kard. Mercierlaan 94, B-3001 Leuven-Heverlee, Belgium

Abstract
A specially adopted finite element (FE) approach for a synchronous reluctance motor with axially laminated rotor is presented. The stator is a standard three phase design. The rotor is constructed by axially interleaved magnetic iron laminations with non-magnetic spacers. Clearly, besides the stator configuration, the rotor construction has more effect on the characteristics of the motors. For both linear and non-linear models, the d-axis and q-axis inductances and their ratio, the maximum torque and power factor, the harmonic analysis of the air gap flux density distribution and the effect of saturation on the torque-current characteristic are evaluated and discussed for a wide range of the air gap variations, the stator excitation current, the thickness of the rotor ferro-magnetic laminations and non-magnetic spacers as well as the rotor saliency factor. The results from the above approach can be used in the rotor design optimisation.

Keywords
Synchronous reluctance machine, finite element method, axially laminated rotor, design, optimisation.

Introduction

Induction and permanent magnet motors are widely used in industrial AC drives because of their high-performance in combination with efficient power converters. Vector control techniques incorporating fast micro-processors made it possible to apply induction motors and permanent magnet motors for high-performance drives where traditionally dc drives were applied.

Permanent magnets with high-energy products have been developed and applied to synchronous motors having high specific torque, low loss/torque ratio, high kW/kVA ratios and fast torque response. Such drives can be equipped with rectangular or sinusoidal current control. However, high manufacturing cost, both for the magnets and the machine itself, restricts their application.

The induction motor is inherently more robust in its construction. The squirrel cage rotor can easily withstand the sharp temperature rise due to high transient torque. However, the specific torque and power factor are lower than the values found in the permanent magnet motors. Also the copper losses are almost twice when compared to the permanent magnet motor. Furthermore, the dynamic behaviour of the field oriented controlled induction motor is less favourable when compared to the permanent magnet motor.

The synchronous reluctance motor drives have some advantages. Compared to the permanent magnet motor they don't have magnets with their operational problems. It is inexpensive to manufacture and can operate at high speed and elevated temperatures. Compared with the induction motor, the exact synchronous speed is one of their advantages. A distinct advantage when used in a vector control scheme is that no rotor parameters have to be identified.

In the past, researchers proposed and improved the structures of an anisotropic rotor of the synchronous reluctance motor such as the segmented rotor, the flux-barrier-rotor and so on [1-10]. D. Platt [11] achieved reluctance motors with strong rotor anisotropy by interleaving magnetic iron laminations with non-magnetic spacer of approximately equal thickness.

In this paper, a specially adopted finite element approach for a synchronous reluctance motor equipped with an axially laminated rotor is presented. The stator has a standard three phase induction motor design. The rotor is constructed with axially interleaved magnetic iron laminations with non-magnetic spacer. In the design stage the calculation of the d-axis and q-axis inductances is the most important part for the performance predictions of the synchronous motor. Clearly, besides the stator configuration, the rotor construction has more effect on the characteristics of the motors. The d-axis, q-axis inductances and their ratio as well as other characteristics of the motor are a function of the air gap length, the rotor salience factor, the thickness of the rotor iron laminations, the rotor non-magnetic insulation and the stator current. Due to the complex construction of the rotor, the finite element method proves to be a powerful tool for the analysis and evaluation of the behaviour of this motor.

2-d mathematical model

Due to the complex shape of the magnetic circuit in the axially laminated rotor, it is very difficult to calculate correctly the parameters using classical electromagnetic analysis method. For the investigation of the operating behaviour of the axially laminated synchronous reluctance motor starting from the analysis of the magnetic field, the finite element method is used. As no time variation or induced currents have to be taken into account, the magnetic flux distribution in the synchronous reluctance motor is determined by computing the time independent, magnetostatic magnetic vector potential. The relative magnetic field equation of the two dimensional model including boundary conditions and assumptions can be found in [12].

d-axis and q-axis inductances

In the design stage, the d-axis and q-axis inductances are the most important parameters for the performance predictions. This is particularly important when introducing the motor in a drive. Defining the saliency factor as the ratio of the rotor span referred to the rotor pitch and the rotor fill-factor as the ratio of the rotor non-magnetic spacer thickness referred to the rotor magnetic lamination thickness, the d-axis and the q-axis inductances as well as their ratio depend on the stator current and its configuration, the air gap length, the rotor saliency factor as well as the rotor fill-factor. With

$$L = \frac{2W_{magn}}{I^2} \tag{1}$$

the inductance can be evaluated. The energy stored in the volume V of an electrical machine is found by integrating the stored magnetic energy density over the volume of the device. The stored energy density is given by the area to the left of its magnetising characteristic:

$$W_{magn} = \int_0^B \vec{H}(b) \bullet d\vec{b} \tag{2}$$

Combining (1) and (2) yields:

$$L = \frac{2}{I^2} \iiint_{system} \left(\int_0^B \vec{H} \bullet d\vec{b} \right) dv \tag{3}$$

In the synchronous reluctance machine, the energy stored in the machine is (See Appendix):

$$W_{magn} = \frac{3}{2}\left(\frac{1}{2}L_d I_d^2 + \frac{1}{2}L_q I_q^2\right) \tag{4}$$

Combining (1), (2), (3) and (4), yields:

$$L_d I_d^2 + L_q I_q^2 = \frac{4}{3} \iiint_V \left(\int_0^B \vec{H}(b) \bullet d\vec{b} \right) dv \tag{5}$$

where

$$(I_d + jI_q) = \frac{2}{3}(I_a + I_b e^{j2\pi/3} + I_c e^{j4\pi/3}) e^{j\theta} \tag{6}$$

Applying a pure d-axis and q-axis current to the field solution, the corresponding d-axis and q-axis problem magnetic field energy is calculated from (5). Furthermore, L_d', L_q' and their ratio as a function of the air gap length, stator current, the rotor salience factor and rotor fill-factor are evaluated.

Linear model For the linear model of synchronous reluctance motors with a rotor saliency factor of 0.67, the d-axis and q-axis inductances L_d' and L_q' (except the end leakage inductance L_σ) as a function of the air gap length (δ) and rotor fill-factor K_{fill} are evaluated and shown in Fig. 1 and Fig. 2.

The main conclusions taken from Fig. 1 and Fig. 2 are:

-For the d-axis (Fig. 1), decreasing the air gap length and the fill-factor of the rotor is productive in terms of an increasing d-axis inductance.

-For the q-axis (Fig. 2), the change of the q-axis inductance is very small when the air gap length increases. It is almost unchanged in case of a rotor fill-factor above 0.4. On the other hand, as the rotor fill-factor increases from 0.2 to 0.4, the decrease of the q-axis inductance is larger. Whereas, this change is smaller with the increasing rotor fill factor from 0.4 to 1.5.

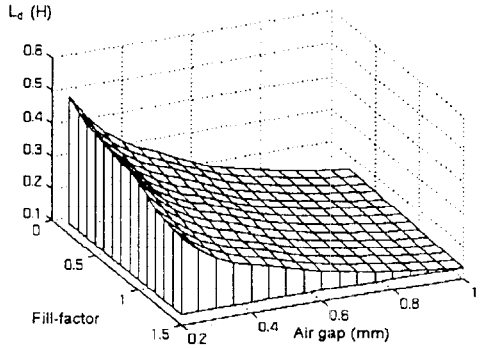

Fig. 1: $L_d'=f(\delta, K_{fill})$ for the linear model

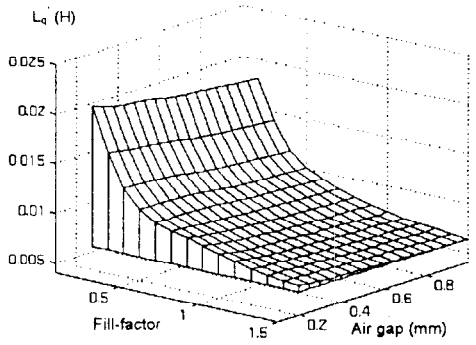

Fig. 2: $L_q'=f(\delta, K_{fill})$ for the linear model

Non-linear models Taking saturation of the magnetic material into account, the d-axis and q-axis inductances L_d', L_q' as well as their ratio L_d'/L_q' as a function of the stator exciting currents (i) and the rotor fill-factor K_{fill} are calculated, with the rotor saliency factor 0.67 and the air gap length 0.35mm (Fig. 3 through Fig. 5).

The main conclusions from the calculated results presented in Fig. 3 through Fig. 5 are:

-For the d-axis inductance, an increasing rotor fill-factor yields a larger equivalent air gap length and the magnetic circuit is not saturated; therefore the variation of the d-axis inductance with the exciting current is small (Fig. 3).

-For the q-axis, due to the flux passing through the longer non-magnetic path including the air gap and the non-magnetic rotor spacers, an increase of the excitation current is hardly productive in terms of variations of the q-axis inductance; on the other hand, the decrease of the q-axis inductance with the rotor fill-factor is smaller when the rotor fill-factor is larger than 0.4 (Fig. 4).

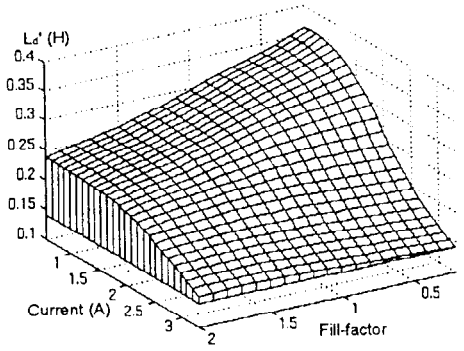

Fig. 3: $L_d'=f(i, k_{fill})$ for the non-linear model

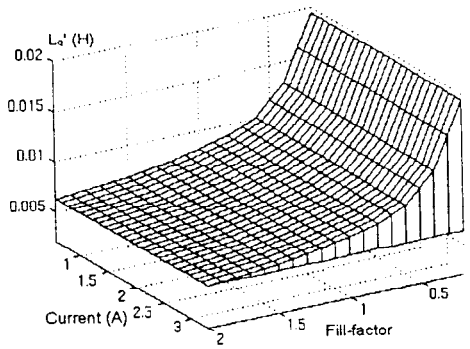

Fig. 4: $L_q'=f(i, k_{fill})$ for the non-linear model

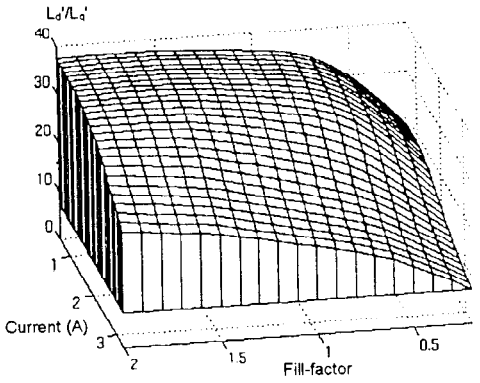

Fig. 5: $L_d'/L_q'=f(i, k_{fill})$ for the non-linear model

Maximum torque and power factor

aximum torque Neglecting the stator resistance, the lative maximum torque T_{max} per Ampère produced by a nchronous reluctance motor without damper winding is:

$$T_{max} = \frac{3}{2}\frac{p}{2}(L_{dm} - L_{qm}) \qquad (7)$$

fact, saturation of the ferro-magnetic material in the odel has to be taken into account when the stator xciting current is large. For the non-linear model and xing the air gap length to 0.35mm, the maximum torque er Ampère T_{max} as a function of the stator current and e rotor fill-factor is evaluated (Fig. 6).

As shown in Fig. 6, the maximum torque per Ampère T_{max} decreases rapidly with increasing excitation current if the fill-factor is smaller than 0.7. For different values of the current, it can be maximised using different rotor fill-factors(for example, stator current of 0.55A yields a rotor fill factor of 0.2, while a stator current of 3.3A yields a rotor fill factor of 1.5). Accordingly, there is a optimum for the current and the fill-factor for the determination of the maximum torque in the design stage.

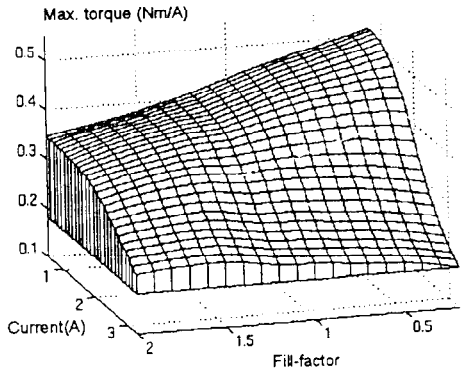

Fig. 6: Specific torque for the non-linear model

Maximum power factor The synchronous reluctance motor is intended to be operated by sinewave currents and therefore, the fundamental power factor cosφ is used:

$$\cos\varphi = \frac{X_d \sin\theta\cos\theta - X_q \sin\theta\cos\theta + R_s}{\sqrt{X_q^2 \sin^2\theta + X_d^2 \cos^2\theta + R_s^2 + 2R_s \sin\theta\cos\theta(X_d - X_q)}} \qquad (8)$$

Neglecting the stator resistance, cosφ has a maximum at

$$\cos\varphi_{max}=(\xi-1)/(\xi+1) \qquad (9)$$

with $\tan\theta=\sqrt{\xi}$ and $\xi = Ld/Lq$.

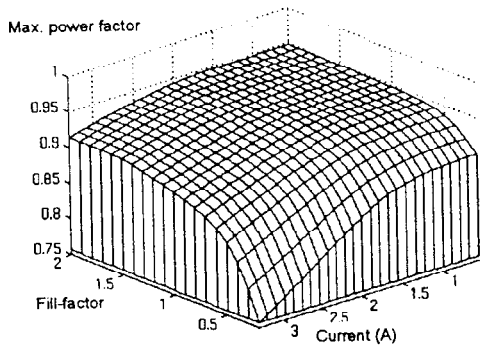

Fig. 7: Max. power factor for the non-linear model

Fig. 7 shows the maximum power factor as a function of the stator current and the rotor fill-factor. The saturation of the ferro-magnetic material is taken into account. Obviously, the larger the fill-factor, the smaller the current and the larger the maximum power factor will be. On the other hand, the maximum power factor decreases rapidly if the current is larger than 2 A and the fill-factor is less than 1.2.

Harmonic analysis of the air gap field

Since any of the harmonic field components in the air gap of the motors acts on the rotor, additional torques, losses and audible noise may occur. It is important to perform a harmonic analysis of the d- and q-axis radial flux density distribution in the air gap. Due to the complex lay-out of the rotor, numerical methods such as finite element method and fast Fourier transformation are used to analyse the d- and q-axis magnetic flux density in the air gap for different saliency factors.

Fig. 8 and Fig. 9 illustrate the case of the fundamental and harmonic components for d-axis and q-axis radial flux density distribution.

It can be seen that for the d-axis air gap flux density distribution, mainly the fundamental component and the stator slot harmonics ($Z_1 \pm 1$ and $2Z_1 \pm 1$ orders) are important. For the q-axis, flux passes through the air gap several times, yielding primarily a leakage flux. The corresponding magnitude of the fundamental component is less than the stator slot harmonics ($Z_1 \pm 1$ and $2Z_1 \pm 1$ orders).

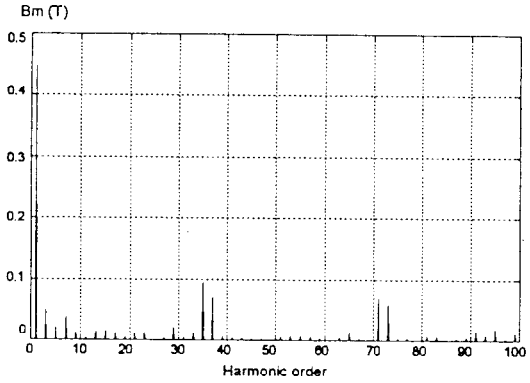

Fig. 8: Harmonic components of the d-axis flux density distribution

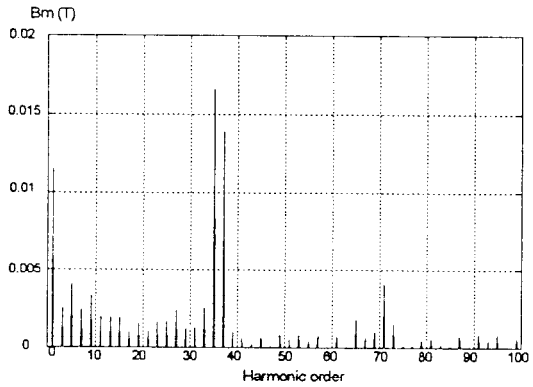

Fig. 9: Harmonic components of the q-axis flux density distribution

Furthermore, the saliency factor of the rotor has a significant effect on the field harmonics. The harmonic ratio is defined as the root mean square of the harmonic components referred to the fundamental component with:

$$R_h = \frac{\sqrt{\sum B_{mv}^2}}{B_{m1}} \qquad (10)$$

Fig. 10 shows the d- and q-axis harmonic ratio for different rotor salience factors of the model with the rotor fill factor of 0.5 and an air gap length of 0.35mm. For the air gap field in the d-axis, the harmonic ratio R_h decreases with an increasing rotor saliency factor. This reduction is small while the saliency factor is larger than 0.66. For the q-axis air gap field, the harmonic ratio R_h has a minimum value when the saliency factor of the rotor is approximately 0.67. This suggests that the rotor saliency factor would be 0.67 in order to reduce the additional torques, the losses and the audible noise produced by the harmonics in the air gap.

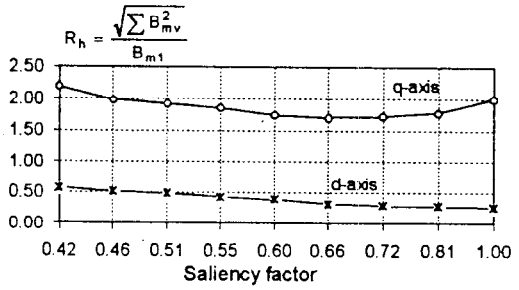

Fig. 10: Ratio of harmonics referred to the fundamental

The effect of the saturation on the torque-current angle characteristic

The torque characteristic describes a major performance of synchronous motor and it can be evaluated in several ways. In order to take saturation into account, the virtual work method is used. It is based on the spatial rate of change of co-energy stored in the synchronous reluctance motor:

$$T = \frac{\Delta W_{co-energy}}{\Delta \theta} \qquad (10)$$

where $\Delta W_{co-energy}$ is the change of the co-energy stored in model and $\Delta\theta$ is the change of the angle. This method is accurate and can be used to calculate the torque of linear and non-linear models, but requires two FE solutions.

Torque-current angle curve with different current As mentioned in the earlier and from the linear magnetic theory, the maximum torque occurs at a current angle of 45^0. However, the maximum torque occurs at values of the current angle larger than 45^0 when saturation of the magnetic materials is taken into account.

Fig. 11 shows the calculated results. The maximum torque occurs at the current angle of 45^0 if the current is smaller than 1A. The maximum torque is found at a current angle of 60^0 if the current is larger than 4A. This is due to the saliency ratio L_d/L_q also being a function of the current angle. For the q-axis, there is almost no saturation in the magnetic field, because the flux mainly passes through a longer air gap and non-magnetic insulation. For the d-axis, the increase in current produces more saturation in the magnetic material. Therefore, for a fixed current, with increasing current angle, the current is rotated towards the q-axis. There is an associated reduction of the d-axis current ($I_d = I\cos\theta$) and reduced saturation. The increased (L_d-L_q) results from reduced

saturation rather it offsets the reduction in the sin2θ term in the analytical torque expression as the current angle increases above 45^0. Accordingly, the maximum torque occurs with a current angles of 45^0 to 60^0 gradually with the increase of the current from 1A to 4A.

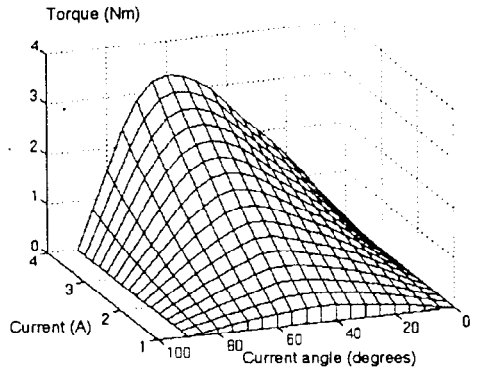

Fig. 11: Torque-current angle curve for different currents

Unit torque-current angle curve Fig. 12 shows the torque per Ampere as a function of the current angle and the current. Due to saturation, the increased current generates smaller values of torque per Ampere. On the other hand, the characteristics of the torque per Ampere becomes progressively closer if the current increases and the current angle is larger than 60^0. Furthermore, if the current angle is larger than 75^0, the torque per Ampere almost does not change while the current increases. The reason for this can be seen for fixed values of the current, a larger current angle means that the current rotates towards the q-axis: the q-axis current I_q increases and the d-axis current I_d decreases. A smaller d-axis current and a larger q-axis current means that there is no saturation in the d- or q-axis respectively. Accordingly, the torque per Ampere curve does not change anymore with increasing current if the current angle is larger than 75^0.

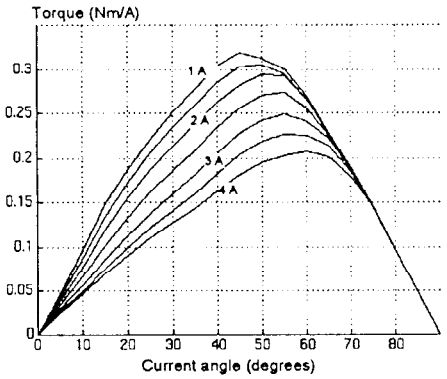

Fig. 12: Torque-current angle characteristic

Conclusions

Some conclusions can be obtained from the computed results by means of finite element approach presented in this paper. The d-axis inductance strongly depends on saturation of the magnetic circuit due to the flux passing through less non-magnetic materials. The q-axis inductance is fairly independent of q-axis current because the flux passes through longer non-magnetic materials including the air gap and the rotor insulation. The harmonic analysis of the air gap field suggests the rotor saliency factor to be 0.67 in order to reduce the additional torques, the losses and the audible noise produced by the harmonics in the air gap. The results from torque calculations show that the saturation of the d-axis field produced by d-axis currents have more effect on the torque current angle curve and the maximum torque. Therefore, there is an optimum for the current and the fill-factor in the design stage for the control of the maximum torque.

Acknowledgements

The authors are indebted to the Belgian Nationaal Fonds voor Wetenschappelijk Onderzoek for its financial support for this work and the Belgian Ministry of Scientific Research for granting the project IUAP No. 51 on Magnetic Fields as well as Katholieke Universiteit Leuven for awarding the scholarship to Mr. Feng.

Appendix

d-q transformation of the phase equation for the sinusoidally supplied synchronous reluctance motor

Mostly, the synchronous reluctance motor is supplied by a three-phase power system. All variables can be expressed in an arbitrary reference frame. A relation between the physical variables (abc-quantities) and the corresponding quantities in the reference frame(e.g. dq-variables) can be found by:

$$\left[V_{dq0s}\right] = \left[T_r\right]\left[V_{abcs}\right] \tag{A1}$$

where:

$$\left[V_{dq0s}\right]^T = \left[V_{ds} \quad V_{qs} \quad V_{0s}\right] \tag{A2}$$

and

$$\left[V_{abcs}\right]^T = \left[V_{as} \quad V_{bs} \quad V_{cs}\right] \tag{A3}$$

The transformation matrix is:

$$\left[T_r\right] = \frac{2}{3}\begin{bmatrix} \cos\theta & \cos(\theta - \frac{2\pi}{3}) & \cos(\theta + \frac{2\pi}{3}) \\ \sin\theta & \sin(\theta - \frac{2\pi}{3}) & \sin(\theta + \frac{2\pi}{3}) \\ \frac{1}{2} & \frac{1}{2} & \frac{1}{2} \end{bmatrix} \tag{A4}$$

with

$$\theta = \int_0^t \omega(\xi)d\xi + \theta(0) \tag{A5}$$

Where ξ is a dummy variable of integration.

In the above equations, V can represent either a voltage, a current, a flux linkage or an electric charge. Here, only currents are required. The magnetic energy at any given instant of time is expressed in abc variables as

$$W_{abcs} = \frac{1}{2}\left[I_{abcs}\right]^T\left[L_{abcs}\right]\left[I_{abcs}\right] \tag{A6}$$

The magnetic energy expressed in the dq0 variables must be equal to the magnetic energy expressed in the abc variables, hence substituting (A1), (A4) into (A6) yields:

$$W_{dq0s} = W_{abcs} = \frac{3}{2}\frac{1}{2}[I_{dq0}]^T[L_{dq0}][I_{dq0}] \qquad (A7)$$

For a three-phase symmetrical circuit, (A7) can be expressed in scalar form:

$$W_{dq0s} = \frac{3}{2}[\frac{1}{2}(L_d I_d^2 + L_q I_q^2)] \qquad (A8)$$

where

$$(I_d + jI_q) = \frac{2}{3}(I_a + I_b e^{j\frac{2\pi}{3}} + I_c e^{-j\frac{2\pi}{3}})e^{j\theta_r} \qquad (A9)$$

with θ_r the angle between the d-axis and the stator phase axis.

References

[1] P. J. Lawrenson and L. A. Agu, 'Theory and performance of polyphase reluctance machines', Proc. IEE, Vol. 111, 1964, pp. 1435-1445.

[2] P. J. Lawrenson, 'Two speed operation of salient-pole reluctance machines', Proc. IEE, Vol. 112, 1965, pp. 2311-2316.

[3] P. J. Lawrenson and S. K. Gupta, 'Developments in the theory and performance of segmental-rotor reluctance machines', Proc. IEE, Vol. 114, 1967, pp. 645-653.

[4] A. J. O. Cruickshank and R. W. Menzies, 'Axially laminated anisotropic rotor for reluctance motors', Proc. IEE, Vol. 113, 1966, pp. 2058-2060.

[5] F. W. Htsui, 'New type of reluctance motor', Proc. IEE, Vol. 117, 1970, pp. 545-551.

[6] J. D. Bak, 'Rotor design minimizes magnetic leakage', Design News, No. 5/21, 1984, pp. 110-111.

[7] T. J. Miller, C. Cossar and A. J. Huttan, 'Design of a synchronous reluctance motor drive', in Proceedings of IEEE-IAS Annual Meeting, 1989, pp. 122-128.

[8] T. A. Lipo, 'Synchronous reluctance machines-a viable alternative for AC drives?', Electrical Machines and Power System, 19, 1991, pp. 659-671.

[9] I. Boldea and S. A. Nasar, 'Emerging electric machines with axially laminated anisotropic rotor', Electrical Machines and Power System, 19, 1991, pp. 673-703.

[10] I. Boldea, Z. X. Fu and S. A. Nasar, 'Performance evaluation of axially-laminated anisotropic (ALA) rotor reluctance synchronous motors', in Proceedings of IEEE-IAS Annual Meeting, Part 1, 1992, pp. 212-218.

[11] D. Platt, 'Reluctance motor with strong rotor anisotropy', IEEE Trans. on Industry Application, Vol. 28, 1992, pp. 652-658.

[12] D. A. Lowther and P. P. Silvester, Computer-Aided Design in Magnetics, New York: Springer-Verlag, 1986.